JOURNAL OF GEOPHYSICAL RESEARCH, VOL. 105, NO. D13, PAGES 17,325–17,340, JULY 16, 2000

A study of gas-aerosol equilibrium and aerosol pH in the remote marine boundary layer during the First Aerosol Characterization Experiment (ACE 1)

A. M. Fridlind and M. Z. Jacobson

Department of Civil and Environmental Engineering, Stanford University, Stanford, California

Abstract. A thermodynamic equilibrium model was applied to study the interactions of gas-phase NH_3, HNO_3, and HCl with size-resolved aerosols and estimate aerosol pH in the remote marine boundary layer during the First Aerosol Characterization Experiment (ACE 1). Analysis of model results and field measurements indicates that accumulation-mode aerosols were probably in equilibrium with NH_3, HNO_3, and HCl simultaneously. The largest coarse-mode aerosols did not appear to be in equilibrium with HNO_3, but may have been in equilibrium with NH_3 and HCl. The estimated pH of accumulation-mode aerosols was 0–2, a function primarily of the amount of sulfate relative to sea salt present in that mode. By contrast, the estimated equilibrium pH of coarse-mode aerosols was 2–5, a function primarily of relative humidity and gas-phase HCl. Prior to exposure to HCl, the estimated pH of fresh sea spray aerosols was 7–9, a function primarily of relative humidity. Sensitivity tests showed that the drying of aerosols during the sampling process may have volatilized up to 30% of NH_4^+.

1. Introduction

Natural and anthropogenic aerosols are believed to play an important role in climate through their direct effect of scattering and absorbing radiation and their indirect effect of serving as cloud condensation nuclei. Measurements and modeling studies have found that marine aerosol components may comprise a significant component of both the direct effect [*Quinn and Coffman*, 1999; M. Z. Jacobson, Global direct radiative forcing due to multicomponent anthropogenic and natural aerosols, submitted to *Journal of Geophysical Research*, 1999] and the indirect effect [*Jones and Slingo*, 1997] of natural aerosols on climate. However, both effects are strongly dependent upon the size, number concentration, and chemical and optical properties of the aerosols [e.g., *Horvath*, 1993]. In order to better quantify the characteristics of natural marine aerosols, the First Aerosol Characterization Experiment (ACE 1) was designed to measure the physical, chemical, and optical properties of aerosols, as well as gas concentrations, in the remote marine boundary layer [*Bates et al.*, 1998a].

Field data indicate that remote marine aerosols, those not significantly affected by either anthropogenic or natural continental sources, are composed primarily of sea salts (Na^+, Cl^-, SO_4^{2-}, Mg^{2+}, Ca^{2+}, K^+, CO_3^{2-}, and Br^-, in order of oceanic molar abundance), nitrate (NO_3^-), ammonium (NH_4^+), non-sea-salt sulfate (SO_4^{2-}), methanesulfonate ($CH_3SO_3^-$), associated hydrogen ions (H^+), and other organics [e.g., *Fitzgerald*, 1991; *O'Dowd et al.*, 1997]. The size distribution is often composed of four modes, including an ultrafine mode, a nucleation or Aitken mode, an accumulation mode, and a sea salt or coarse mode [e.g., *Bates et al.*, 1998b; *O'Dowd et al.*, 1997]. During ACE 1, in terms of dry geometric diameter, these modes were observed at 5–20 nm, 20–80 nm, 80–300 nm, and >300 nm, respectively, in the number size distribution [*Bates et al.*, 1998b]. Aside from aerosol mass advected from continents or entrained from the free troposphere, the mass is produced exclusively by sea spray emissions and gas-to-particle conversion. Sea spray aerosols are emitted directly by ocean surface disturbances at both accumulation-mode and coarse-mode sizes, and may be enriched upon emission with oceanic surface active organic compounds [e.g., *Barger and Garrett*, 1970; *Middlebrook et al.*, 1998]. All other significant components of soluble mass (NH_4^+, NO_3^-, non-sea-salt SO_4^{2-}, $CH_3SO_3^-$, and perhaps additional organic species) are secondary, resulting from gas-to-particle conversion processes. Such processes include nucleation, condensation, dissolution, and aqueous-phase oxidation of dissolved intermediates. Whereas ambient NH_3 is accumulated as NH_4^+ primarily by the acidic sulfate aerosols, ambient HNO_3 is accumulated as NO_3^- primarily by the less acidic sea spray aerosols. When acids are added to aerosols containing sea salt, Cl^- may be displaced as HCl, which may in turn be scavenged by fresh sea spray, enhancing Cl^- in those particles [e.g., *Erickson et al.*, 1999]. A host of other physical processes influences the boundary layer concentration and chemical characteristics of the marine aerosol population, including coagulation, dry deposition, sedimentation, cloud formation, precipitation scavenging, horizontal advection, and vertical exchange with the free troposphere.

Within this environment the nature of the partitioning of chemical species between the gas and aerosol phases depends upon the characteristics of the aerosol population, the characteristics of the species, and the degree of gas-aerosol equilibrium obtained. Many gases may interact reversibly with the aerosol phase, including NH_3, HNO_3, HCl, CH_3SO_3H, HCOOH, CH_3COOH, SO_2, and O_3. Among these, only NH_3, HNO_3, and HCl have been proven to interact with a reservoir in the aerosol phase that has been observed to comprise a significant fraction of total aerosol mass in remote marine regions [e.g., *Parungo et al.*, 1986; *Quinn et al.*, 1992], thereby exerting significant reversible influence on aerosol physical, chemical, and optical properties.

Copyright 2000 by the American Geophysical Union.

Paper number 2000JD900209.
0148-0227/00/2000JD900209$09.00

Limited evidence from remote marine air masses indicates that HCOOH and CH_3COOH may also fall into this category [e.g., *Matsumoto et al.*, 1998], but neither was measured during ACE 1, and sensitivity tests indicated that they would not be expected to contribute significant aerosol mass at equilibrium under ACE 1 conditions. Current field data indicate that remote marine aerosols that are not fully neutralized are likely to be in equilibrium with ambient NH_3 [*Quinn et al.*, 1992], a result supported by modeling studies of ACE 1 aerosols [*Quinn et al.*, 1998] and prototypical aerosols under more polluted conditions [*Meng and Seinfeld*, 1996]. By contrast, field data gathered under polluted conditions indicate that smaller sea spray aerosols are likely to be in equilibrium with ambient HNO_3 and HCl whereas larger aerosols may not be [*Keene and Savoie*, 1998, 1999]. This observation has also been supported under some conditions by a modeling study [*Erickson et al.*, 1999].

Solution pH is an important characteristic of aerosols that may be closely associated with gas-aerosol equilibrium. The pH of remote marine aerosols may be critical to aqueous-phase chemistry in the marine boundary layer [e.g., *Chameides and Stelson*, 1992; *Clegg and Toumi*, 1997; *Keene et al.*, 1998; *Sievering et al.*, 1992], but few efforts have been made to determine aerosol pH since it is extremely difficult to reliably estimate from measurements [*Keene and Savoie*, 1998]. Previous estimates have been based upon indirect observation of marine aerosols or models of prototypical aerosols (Table 1). Estimated pH values under remote marine conditions have ranged from -1 to 3 in the accumulation mode and 2–10 in the coarse mode.

The goals of this study were to apply a thermodynamic equilibrium model to the size-resolved aerosol field data gathered during ACE 1 in order (1) to estimate whether aerosols were equilibrated with gas-phase NH_3, HNO_3, and HCl; (2) to test the sensitivity of gas-aerosol equilibrium to the aerosol sampling process (aerosols were heated and dried during sampling) in order to ascertain whether volatile material shifted phase due to the sampling process; and (3) to estimate the pH of the aerosols.

Table 1. Estimates of Marine Aerosol pH Based on Indirect Observations or Model Results

pH	Conditions	Method	Source
Accumulation mode			
1–3	remote	observation	*Winkler* [1986]
0–2	remote	model	this work
-1–1	continental	model	*Zhu et al.* [1992]
-1–0	remote	model	*Katoshevski et al.* [1999]
Coarse mode			
6–10	remote	model	*Katoshevski et al.* [1999]
6–9*	remote	observation	*Winkler* [1986]
5–8	remote	model	*Erickson et al.* [1999]
5–6	remote	model	*Keene et al.* [1998]
5–6	remote	model	*Vogt et al.* [1996]
3–5	remote	model	*Chameides and Stelson* [1992]
3–5	continental	observation	*Keene and Savoie* [1999]
2–6	continental	model	*Sander and Crutzen* [1996]
2–5	remote	model	this work
2–5	continental	model	*Erickson et al.* [1999]
-1–12	continental	model	*Zhu et al.* [1992]

Marine conditions were designated as approximately either "remote," meaning free of anthropogenic or natural continental influence, or more "continental."

*Values obtained from leaching solutions of marine aerosols.

Table 2. Range and Median of Measurements

Variable	Range	Median
Aerosol mass, ng m^{-3}		
Na^+	1040–6510	2160
Mg^{2+}	197–999	407
Ca^{2+}	106–837	214
K^+	39.6–293	90.6
NH_4^+	7.2–43.7	19.5
Cl^-	1510–10,900	3440
Br^-	0–72.0	17.9
SO_4^{2-}	453–1750	812
$CH_3SO_3^-$	18.2–221	36.0
NO_3^-	6.93–77.0	40.1
NH_3, ppt	3–46	8
Pressure, mb	993–1024	1009
Temperature, °C		
Ambient	4–13	10
Sample	16–24	22
Relative humidity, %		
Ambient	61–97	76
Sample	26–44	37

2. Data

Aerosol, gas, and meteorological measurements were made over the Southern Ocean (40°–55°S, 135°–160°E) between November 18 and December 11, 1995, on the National Oceanic and Atmospheric Administration (NOAA) R/V *Discoverer* ship. This segment of the ACE 1 experiment was chosen due to the availability of NH_3 measurements, and all 19 aerosol samples that were collected during the segment were included in this study.

2.1. Aerosol Data

Aerosols were measured with a seven-stage Berner-type cascade impactor, as described by *Quinn et al.* [1998]. Ion chromatography was used to determine total soluble Cl^-, Br, NO_3^-, SO_4^{2-}, $CH_3SO_3^-$, Na^+, NH_4^+, K^+, Mg^{2+}, and Ca^{2+}. A mass closure study using other data gathered on the *Discoverer* concluded that these ions accounted for all aerosol mass within experimental uncertainty [*Quinn and Coffman*, 1998], indicating that organics and insoluble dust were not a dominant component. The samples were collected from an inlet approximately 18 m above sea level and dried by heating prior to entering the impactor. Mean aerodynamic diameters at the dry sample relative humidity were 0.15, 0.32, 0.49, 0.89, 1.7, 3.3, and 7.4 μm, resolving the accumulation and coarse aerosol modes. Sample exposure periods were 16–40 hours, corresponding to an average sample volume of 26 m^3. The range and median of the aerosol measurements (summed over the impactor stages) are shown in Table 2. Of the 19 aerosol samples collected, 4 samples were significantly continentally influenced (samples 32–34 and 36), as defined by 2-hour mean radon concentrations exceeding 100 mBq m^{-3}, and the remaining 15 samples were more representative of pure maritime air [*Whittlestone et al.*, 1998].

2.2. Gas Data

Gas data used were measured CO_2 and NH_3, and estimated HNO_3 and HCl. CO_2 was collected from an inlet approximately 13 m above sea level and an average representative value of 360 ppm was used for all samples. NH_3 was measured from an inlet approximately 17 m above sea level, with a sample exposure period of 48 to 84 hours, as described by *Quinn et al.* [1998]. The range and median of the measurements are included in Table 2.

Since HNO_3 and HCl measurements were unavailable, their concentrations were estimated from other data sets. HNO_3 was estimated as 10 ppt, the mean summertime value measured under clean marine conditions on the coast of New Zealand at 41°S, 175°E [*Allen et al.*, 1997]. Other measurements of HNO_3 in the marine boundary layer in the Southern Hemisphere are comparable, with a mean of less than 30 ppt measured at 0°–30°S over the Atlantic Ocean [*Papenbrock et al.*, 1992]. HCl was estimated as 100 ppt, a typical low value measured in boundary layer air under clean marine conditions [*Graedel and Keene*, 1995; *Kajii et al.*, 1997; *Pszenny et al.*, 1993; *Singh*, 1995]. The sensitivity of the results to the estimated HNO_3 and HCl concentrations is addressed below in sections 4.2 and 4.3.

2.3. Meteorological Data

Ambient meteorological data used were 30-min average pressure, temperature, and relative humidity, collected from instruments located approximately 13 m above sea level. Temperature and relative humidity were also monitored in the heated aerosol sampling line. All meteorological variables were averaged over each aerosol sampling period to obtain representative values. The range and median of the representative values are included in Table 2.

3. Gas-Aerosol Equilibrium Model

The following provides a description of the gas-aerosol equilibrium model that was applied to the data. A conceptual overview is first given, followed by a technical description, a summary of the initial conditions, and a discussion of the primary assumptions.

3.1. Conceptual Overview

Observed gas and size-resolved aerosol species were assumed to be in thermodynamic equilibrium at observed temperatures, pressures, and relative humidities. The thermodynamic equilibrium of the gas-aerosol system can be conceptualized as the result of the competitive demand of the nonvolatile species in each aerosol size bin for the available volatile compounds in the system. The nonvolatile aerosol species cannot migrate among the size bins, and thus their predicted size distributions always equal their initial distributions. However, the volatile aerosol species may migrate among the various aerosol size bins via the gas phase until equilibrium has been obtained. Thus the predicted size distributions of the volatile species may differ from the measurements with which they were initialized. Deviations between the predicted and measured aerosol size distributions of the volatile species result from three general sources of error: (1) error in the model assumptions (e.g., lack of actual equilibrium between the gas and aerosol phases), (2) error in the model calculations (e.g., error in the estimated water uptake of sea salts), or (3) error in the estimated or measured concentrations of gases or aerosols (e.g., experimental uncertainty in measured Cl^- concentration).

In this study, the thermodynamic equilibrium of the gas-aerosol system was calculated under the ambient conditions in the marine boundary layer (high relative humidity and low temperature) and also under the sampling conditions in the particle impactor (low relative humidity and higher temperature). The equilibrium gas-aerosol partitioning of the volatile aerosol species may be especially sensitive to changes in the relative humidity of the system due to the concomitant change in the liquid water content of the aerosols.

3.2. Technical Description

The EQUISOLV II model applies the Zdanovskii-Stokes-Robinson equation to estimate liquid water content and Bromley's method to estimate mean mixed activity coefficients [*Jacobson*, 1999a, b]. Additional thermodynamic data added to the model for this study were the 25°C dissociation, water activity, and binary activity coefficients applicable to CH_3SO_3H(aq) solution [*Clegg and Brimblecombe*, 1985; *Covington et al.*, 1973]. Gas-phase species considered were H_2O, CO_2, NH_3, HNO_3, and HCl. Aerosol-phase species considered were H_2O(aq), H_2CO_3(aq), H_2SO_4(aq), CH_3SO_3H(aq), NH_4^+, Na^+, Mg^{2+}, Ca^{2+}, K^+, H^+, NO_3^-, HSO_4^-, SO_4^{2-}, Cl^-, Br^-, $CH_3SO_3^-$, HCO_3^-, CO_3^{2-}, NH_4NO_3(s), NH_4Cl(s), NH_4HSO_4(s), $(NH_4)_2SO_4$(s), $(NH_4)_3H(SO_4)_2$(s), NH_4HCO_3(s), $NaNO_3$(s), NaCl(s), $NaHSO_4$(s), Na_2SO_4(s), $NaHCO_3$(s), Na_2CO_3(s), KNO_3(s), KCl(s), $KHSO_4$(s), K_2SO_4(s), $KHCO_3$(s), K_2CO_3(s), $Ca(NO_3)_2$(s), $CaCl_2$(s), $CaSO_4$(s), $CaSO_4$–$2H_2O$(s), $CaCO_3$(s), $MgCl_2$(s), $Mg(NO_3)_2$, $MgSO_4$(s), and $MgCO_3$(s).

The inputs for each sample were aerosol mass concentrations, gas concentrations, and meteorological variables. Aerosol inputs were the observed soluble mass of Na^+, Cl^-, Ca^{2+}, Mg^{2+}, K^+, Br^-, SO_4^{2-}, $CH_3SO_3^-$, NH_4^+, and NO_3^- in each of the seven size bins. Initial charge imbalances in each size bin were attributed to unmeasured H^+ and CO_3^{2-}. Gas-phase inputs were observed CO_2 and NH_3, and estimated HNO_3 and HCl. Meteorological inputs were observed pressure, temperature, and relative humidity (either in the marine boundary layer or in the particle impactor).

Model outputs were the equilibrium concentration of all gas species and the concentration of each aqueous, ionic, and solid component in each size bin of the aerosol phase, including equilibrium water content and pH. The total soluble mass of a compound was then calculated as the sum of its liquid, ionic, and solid concentrations in order to compare it with observations. For example, the total soluble SO_4^{2-} would be the sum of the SO_4^{2-} mass predicted as H_2SO_4(aq), HSO_4^-, SO_4^{2-}, NH_4HSO_4(s), and all other solids containing sulfate.

Since multiple size bins were used, the thermodynamic equilibrium solution was unique only if no solids were predicted that contained two volatile species (i.e., NH_4NO_3(s), NH_4Cl(s), or NH_4HCO_3(s)) [*Jacobson*, 1999b]. Such solids were never predicted in the ACE 1 samples, permitting a unique solution in all cases.

All aerosol field data were reported as functions of the mean aerodynamic diameter at the sampling relative humidity, and this value was assumed to be the initial geometric diameter of the model size bin under both ambient and sampling conditions. Model results indicated that geometric diameter did not typically deviate from the mean aerodynamic diameter by more than 8% and dry geometric diameter did not typically deviate from it by more than 30%. Furthermore, model results were independent of the bin size specification since Kelvin effects are small for particles larger than ~0.1 μm diameter [e.g., *Jacobson*, 1999a]. All field data and model predictions are reported here as a function of the dry aerodynamic diameter.

3.3. Initial Conditions

The observed gas-aerosol systems were first considered at the pressures, temperatures, and relative humidities observed in the marine boundary layer (section 2.3). Gases were initialized as

measured or estimated (section 2.2). In the aerosol phase each of the 19 aerosol samples was first initialized with the observed species in each size bin (section 2.1). However, experimental uncertainty in the major sea-salt ions often created large charge imbalances and discontinuities in pH from one size bin to the next. Thus each of the 19 aerosol samples was also initialized using a charge-balancing procedure: Cl^-, Mg^{2+}, Ca^{2+}, K^+, and sea-salt SO_4^{2-} were also scaled to measured Na^+ using standard sea-salt composition [*Stumm and Morgan*, 1996]; Br^- was not permitted to exceed the sea-salt Br^-:Na^+ ratio, but was not raised if it was depleted [e.g., *Ayers et al.*, 1999]; and all of the secondary species, including non-sea-salt SO_4^{2-} (defined as that exceeding the sea-salt ratio to Na^+), $CH_3SO_3^-$, NH_4^+, and NO_3^-, were unchanged. Initializing with the charge-balancing procedure preserved the primary characteristics of the marine aerosols and eliminated the primary influence of experimental uncertainty on the results.

In addition to modeling the 19 ACE 1 samples, two prototypical samples were derived to represent the behavior of generic remote marine aerosols. First, an idealized sample was derived from the clean marine samples by using the median values of measured meteorological inputs, NH_3, Na^+, $CH_3SO_3^-$, NH_4^+, NO_3^-, and non-sea-salt SO_4^{2-}, and scaling Cl^-, Ca^{2+}, Mg^{2+}, K^+, Br^-, and sea-salt SO_4^{2-} to the median Na^+ in each size bin (Figure 1). Second, a pure sea-salt sample was derived by removing all secondary species ($CH_3SO_3^-$, NH_4^+, NO_3^-, and non-sea-salt SO_4^{2-}) from the ideal sample.

Simultaneous equilibrium with all gases was modeled for the ideal and sea-salt samples, as well as for the 19 ACE 1 samples using both charge-imbalanced and charge-balanced data. The charge-balanced data were considered more representative of actual conditions; however, the results using charge-imbalanced data are also included here in order to entirely establish the impact of the charge-balancing procedure.

Several sensitivity tests were then performed on the charge-balanced, ideal, and sea-salt samples. The sensitivity of the gas-aerosol partitioning to the ambient gas concentrations was tested by initializing each gas to a minimum value of zero and a maximum value of twice its measured or estimated concentration. The sensitivity of the gas-aerosol partitioning of NH_3, HNO_3, and HCl to the heated, dry sampling conditions was tested by setting temperature and relative humidity to values representative of the sampling conditions (section 2.3). Finally, the sensitivity of the ideal and sea-salt samples to independent equilibration with NH_3, HNO_3, and HCl was tested to elucidate the role of each gas in controlling aerosol pH.

3.4. Model Assumptions

Applying the model to the available data involved a number of important assumptions regarding (1) the simplification of the physical gas-aerosol system (particles were uniform and internally mixed), (2) the properties of the observations (gases and aerosols were stationary in time, gas-aerosol partitioning was insensitive to the aerosol sampling process), and (3) the thermodynamic state of the gas-aerosol system (particles were or were not deliquescent, gas-aerosol equilibrium was obtained). Because these assumptions are important to the interpretation of the model results, they are discussed here in detail prior to presentation of results in section 4.

3.4.1. Uniform internal mixture. Particles on a given impactor stage were assumed to be a well-mixed internal mixture of the measured species. This was probably a good assumption in the coarse mode, but perhaps sometimes less accurate in the accumulation mode. Two distinct types of particles, sea-salt particles and ammonium-sulfate particles, have been found to dominate the aerosol in remote marine regions according to analysis by single-particle methods [*Gras and Ayers*, 1983; *McInnes et al.*, 1994], hygroscopic growth [*Berg et al.*, 1998] and volatility [*Kreidenweis et al.*, 1998]. These two types correspond to the two dominant sources of remote marine particles discussed above: sea spray and nucleation. Whereas essentially all of the coarse-mode particles have been found to be sea salt [*Pósfai et al.*, 1995; *Gras and Ayers*, 1983; *Kreidenweis et al.*, 1998], a mixture of separate sea-salt and ammonium-sulfate particles has been observed in the accumulation mode [*Berg et al.*, 1998; *Gras and Ayers*, 1983; *Kreidenweis et al.*, 1998]. However, evidence has also indicated that almost all accumulation-mode aerosols larger than 0.13 μm may contain sea salt [*Murphy et al.*, 1998].

In the accumulation mode, deviations from uniformity may be important to gas-aerosol interactions because an internal mixture of non-sea-salt sulfate with sea salt may behave very differently from an external mixture. Specifically, an equimolar internal mixture of aqueous NH_4HSO_4(s) and NaCl(s) would emit essentially all Cl^- and NH_4^+ as HCl and NH_3 under typical ACE 1 conditions, whereas an equimolar external mixture would retain both

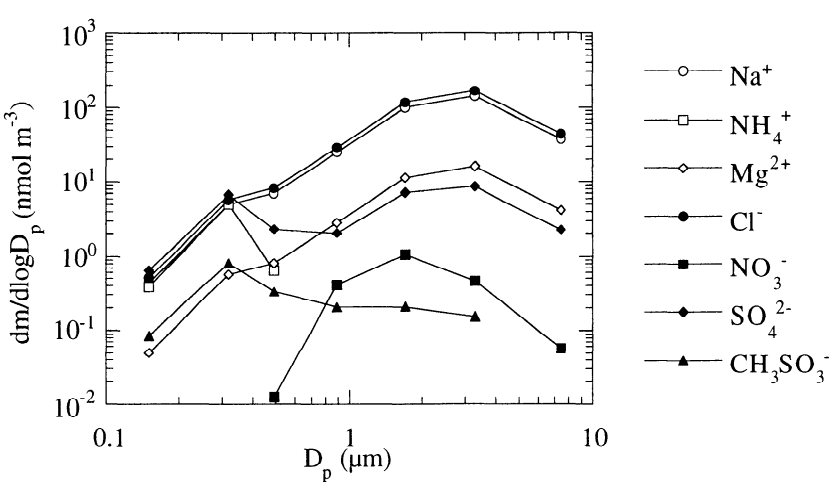

Figure 1. Size distribution of aerosol species in the ideal sample (Ca^{2+} and Br^- not shown).

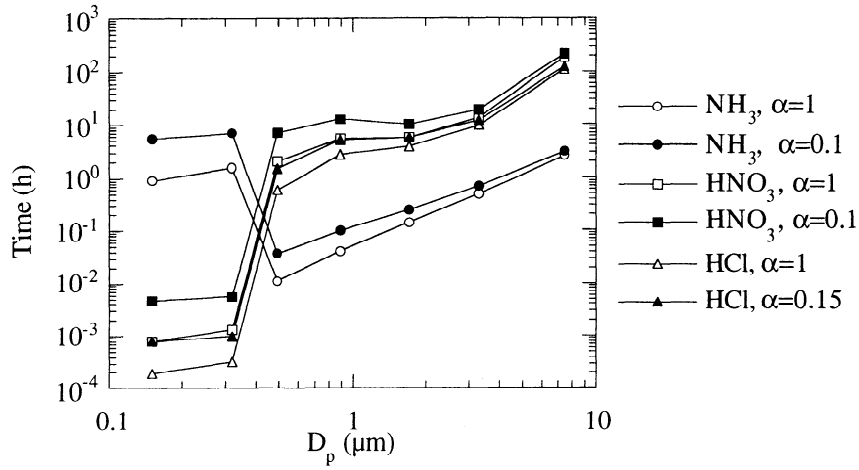

Figure 2. Calculated time required for aerosols to obtain 95% equilibration with a given gas as a function of the accommodation coefficient of the gas, α.

species. This behavior has been verified by individual particle data in the marine boundary layer with respect to HCl emission [e.g., *McInnes et al.*, 1994]. During the ACE 1 period studied here, hygroscopicity data gathered on the *Discoverer* indicated that a range of 0–80% of the 0.165-μm particles were externally mixed sea salt [*Berg et al.*, 1998]. However, data were not gathered at larger particle sizes, where the accumulation-mode mass was concentrated.

3.4.2. Stationarity. For modeling purposes, the gas and aerosol mass concentrations were assumed to be constant during the time that each aerosol sample was collected. However, gas and aerosol concentrations may have varied significantly during aerosol sampling periods. Other data sets provide evidence for diurnal and air mass variations in HNO_3 and HCl [*Keene et al.*, 1993; *Papenbrock et al.*, 1992]. Particle size distributions measured on the *Discoverer* during sampling also indicated that the aerosol population was not constant over the long impactor sampling periods [*Bates et al.*, 1998b]. The deviations of predictions from measurements due to the inaccuracy of this assumption were not quantified due to lack of data describing short-term deviations in gas and ionic mass encountered.

3.4.3. Humidity-insensitive partitioning. The measured gas and volatile particulate mass concentrations were assumed to be valid under both sampling and ambient conditions. However, the sampling process (heating and drying) may have volatilized some aerosol species (such as NH_4^+ or NO_3^-). If volatilization took place, the ambient gas concentration plus the sampled aerosol concentration of a given volatile compound would represent an underestimate of the total volatile mass actually present in the marine boundary layer. The possible extent of this underestimate under ACE 1 conditions is quantified in sections 4.1–4.3.

3.4.4. Solid formation. Under ambient conditions the requirement of homogeneous solid formation was considered to discourage solid formation above the crystallization relative humidity (CRH). Solids were assumed to form only below their CRH, and no solids were predicted in any sample. However, under the dry sampling conditions on the impactor substrates, heterogeneous solid formation on the substrate media was assumed to permit solids to form close to their deliquescence relative humidity (DRH). Solids were then assumed to form when the relative humidity fell below their DRH, and solids predicted to form in some samples included $(NH_4)_2SO_4(s)$, $(NH_4)_3H(SO_4)_2(s)$, NaCl(s), $Na_2SO_4(s)$, KCl(s), $K_2SO_4(s)$, $CaSO_4{-}2H_2O(s)$, $MgSO_4(s)$, and $MgCO_3(s)$. Sensitivity tests indicated that these assumptions generally had negligible influence on the results except in the three cases where significant $CaSO_4{-}2H_2O(s)$ influenced the predicted partitioning of nitrate at the dry sampling relative humidity, as discussed in section 4.2.

3.4.5. Gas-aerosol equilibrium. Gas-aerosol equilibrium was assumed by the model for all gases present. Whereas the equilibration of aerosols with atmospheric water vapor and CO_2 is generally fast due to the high concentrations of those gases, equilibration with trace gases at lower concentrations may take much longer. Gas-aerosol equilibrium may not always have been obtained by the majority of particles of a given size under ACE 1 conditions.

An upper limit to the independent equilibration time of each aerosol size bin of the ideal sample with each ambient gas was estimated with the method used by *Jacob* [1985] for cloud drops, except that model-calculated gas-aerosol partitioning was used in place of the effective Henry's law coefficients in order to account for the activity coefficients in concentrated aerosol solutions [e.g., *Quinn et al.*, 1992]. The equilibration times (Figure 2) represent the approximate time required to reach 95% equilibration of the aqueous phase during a diffusion-limited transfer process. For example, if all of the equilibrium NH_4^+ in a given size bin were instantaneously displaced to the gas phase, the equilibration time would be the time required for the particle to reabsorb 95% of the displaced gas. A range of gas accommodation coefficients was used due to uncertainty in the values. The accommodation coefficient of HCl over a water surface has been measured as 0.15, while a typical range of 0.1–1 was used for NH_3 and HNO_3 due to lack of data [*Seinfeld and Pandis*, 1998, and references therein]. Measurements of HNO_3 uptake by aqueous NaCl(s) particles suggest that the accommodation coefficient is likely to be relatively large [*Abbatt and Waschewsky*, 1998]. Similarly, measurements of NH_3 uptake by sulfuric acid solutions suggest that the accommodation coefficient may increase from ~0.1 to near unity as solution acidity increases [*Swartz et al.*, 1999].

Overall, the results suggest that accumulation-mode aerosols in the smallest three size bins equilibrated with all gases within ~10 hours, a time that was probably significantly shorter than the mean lifetime of the particles in that size range. Whereas all of the larger particles were also likely to be in equilibrium with

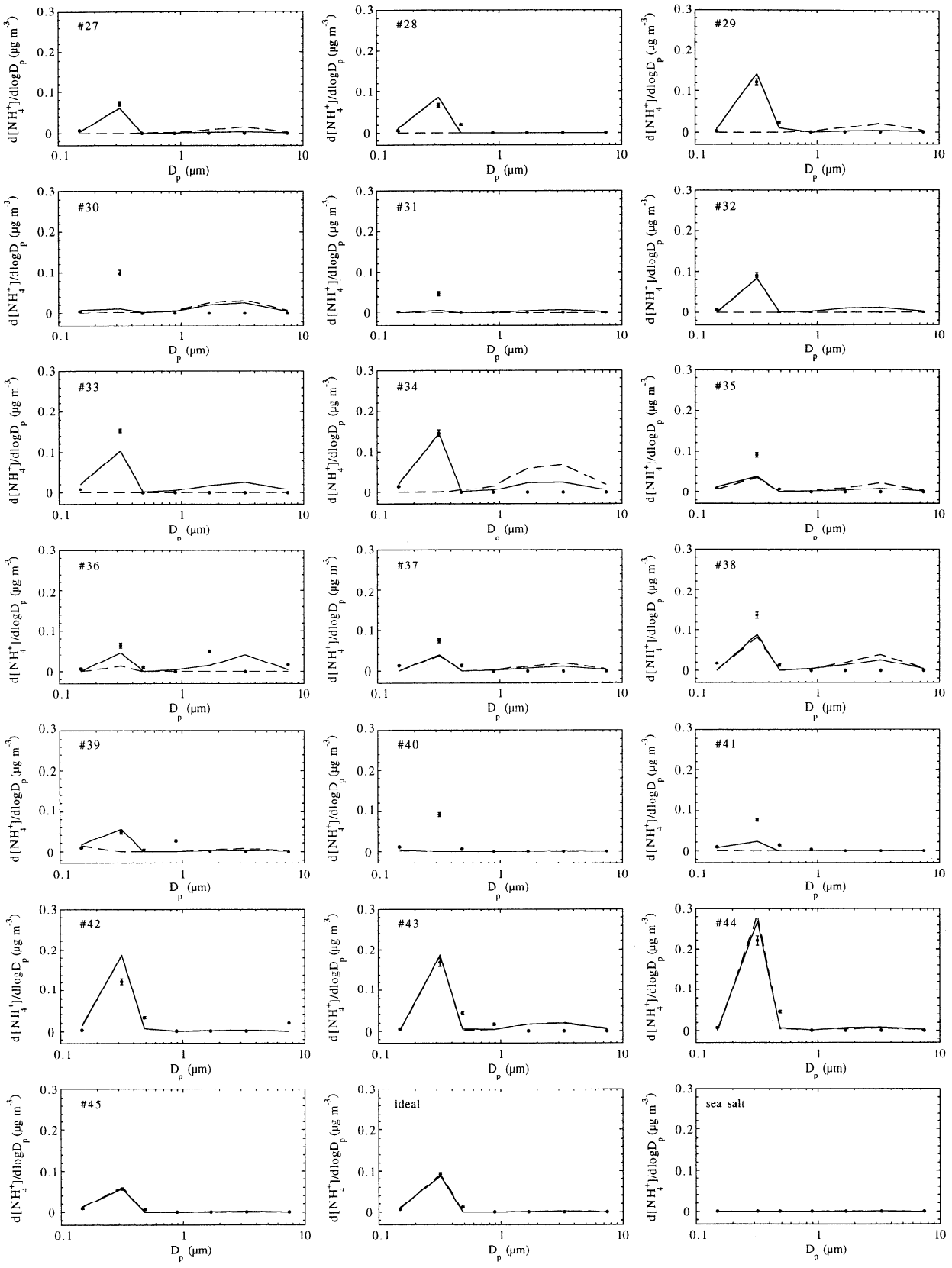

Figure 3. Comparison of observed NH_4^+ (circles with uncertainty bars) with calculated NH_4^+ using charge-imbalanced data (dashed lines) and charge-balanced data (solid lines).

NH_3, estimated equilibration times with HNO_3 and HCl were ~10–300 hours, times that may have been on the order of the mean lifetime of the larger particles. Thus, whether the particles larger than ~0.89 μm were in equilibrium with HNO_3 and HCl may have depended upon their lifetimes, which in turn may have varied significantly across the coarse mode due to differential loss rates by sedimentation and dry deposition [e.g., *Slinn and Slinn*, 1980].

4. Results

Model results for aerosol equilibrium with each gas, NH_3, HNO_3, and HCl, are analyzed in sections 4.1–4.3. The modeled pH of the aerosols is then analyzed in section 4.4.

4.1. Aerosol Equilibration With NH_3

Overall, the acidic sulfates in the accumulation mode had the greatest demand for the available ammonia in the system, whereas the less acidic sea salts in the coarse mode had the least demand (Figure 3). The generally good match between charge-balanced calculations and observations, combined with the short expected equilibration times (Figure 2), suggests that the aerosols were probably in equilibrium with NH_3. Using a different model and assuming a fully external mixture of sea salts and non–sea-salt SO_4^{2-}, *Quinn et al.* [1998] also concluded that aerosols appeared to be in equilibrium with NH_3 during ACE 1.

4.1.1. Accumulation-mode NH_4^+. In the accumulation mode, NH_4^+ was commonly underpredicted (Figure 3), and the degree of underprediction was closely correlated with increasing concentrations of sea salt relative to sulfate (Figure 4). Physically, HCl was released from the particles containing sea salt, increasing pH and reducing the demand of the particles for NH_4^+. However, it is likely that accumulation-mode particles were actually in equilibrium with both NH_3 and HCl (Figure 2). Why, then, did equilibrium predictions deviate from observations in some samples?

The reason for underprediction of accumulation-mode NH_4^+ cannot be conclusively determined here. The three general types of error that may occur, as discussed in section 3.1, include error in model assumptions, error in model calculations, and error in initialized values. With respect to model assumptions, it is noted

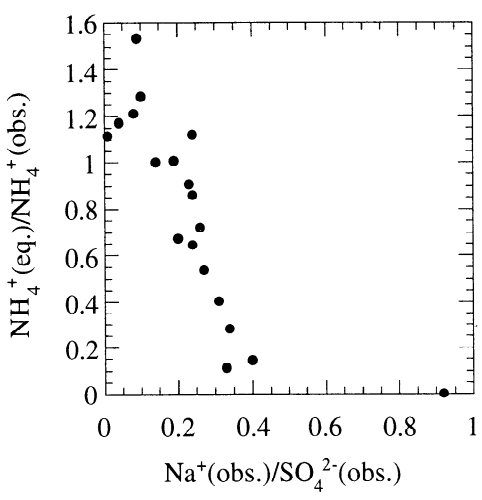

Figure 4. Ratio of calculated equilibrium NH_4^+ to observed NH_4^+ in the 0.32-μm size bin as a function of the ratio of observed Na^+ to SO_4^{2-} in that size bin on a mass basis.

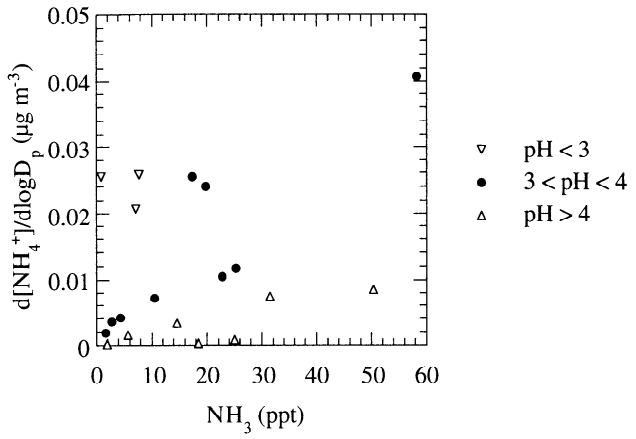

Figure 5. Calculated NH_4^+ in the 3.4-μm size bin as a function of equilibrium NH_3 and pH in that size bin.

that any degree of deviation from the assumed uniform internal mixture of sea salt with non-sea-salt sulfate would result in underprediction of NH_4^+ by the model. With respect to error in model calculations, the EQUISOLV II model has been compared with the AIM2 and SCAPE2 models for the behavior of the fundamental Na^+–Cl^-–NH_4^+–SO_4^{2-} system encountered here [*Zhang et al.*, 1998], and the AIM2 model has in turn been compared with copious laboratory data [*Clegg et al.*, 1998], making significant model error unexpected. With respect to error in measurements, it is not immediately expected that the error would be significantly skewed to result in underprediction of accumulation-mode NH_4^+. In summary, the physical cause of underestimated submicron NH_4^+ was the assumed internal mixture of large quantities of sea salt with the accumulation-mode SO_4^{2-} (Figure 4). However, it cannot be corroborated that some degree of external mixture or nonuniformity among the particles was actually responsible for the deviation between model results and observations.

4.1.2. Coarse-mode NH_4^+. In the coarse mode, observations indicated that the sea-salt aerosols had little demand for NH_4^+, but significant equilibrium NH_4^+ was predicted in about one third of the samples (Figure 3). This was closely correlated with two factors: (1) high equilibrium NH_3 gas and (2) low equilibrium pH in the coarse mode (Figure 5).

High equilibrium NH_3 did not appear to explain the discrepancy between predictions and observations. NH_3 concentrations >20 ppt were measured during six samples (samples 31–36), but NH_4^+ was rarely measured in the coarse mode. Furthermore, lack of equilibrium with the gas phase did not appear to explain this discrepancy between model results and observations. When the equilibration times in Figure 2 were adjusted to account for uptake of significant NH_3 by the coarse mode, the equilibration time of all except the largest size bin remained less than 10 hours and less than the equilibration times with HNO_3, which had sufficient time to accumulate significantly as NO_3^-.

Low estimated pH in the coarse mode appeared more likely to explain instances of overpredicted NH_4^+ in the coarse mode. As discussed below (section 4.4), modeled coarse-mode pH was controlled by equilibration with HCl at a given relative humidity. Consistent with this finding, two changes in the initial conditions raised equilibrium pH above 3.5 and eliminated the equilibrium coarse-mode NH_4^+ in all charge-balanced samples: (1) reducing relative humidity to 65% and (2) reducing equilibrium HCl below 65 ppt in all cases, which required removing all initial HCl as

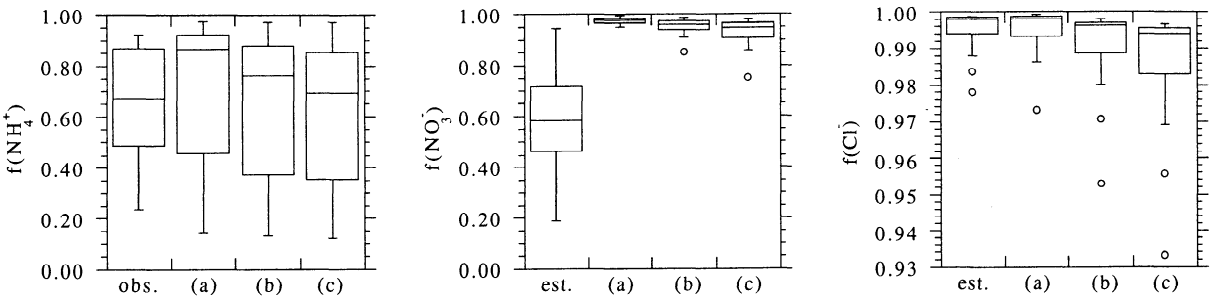

Figure 6. Comparison of the observed or estimated particulate fraction with that calculated in equilibrium with initial gas concentrations of (a) zero, (b) observed or estimated values, and (c) double the observed or estimated values. Boxes span 25% of the data points above and below the median, with whiskers and outliers indicating the range of the remaining data.

well as 2–4% of the initial Cl^-. This leads to the possible conclusions that (1) NH_4^+ was present at the ambient relative humidity but was volatilized during the measurement procedure or (2) ambient HCl was less than ~65 ppt. Furthermore, the model results indicate that an equilibrium value of 65 ppt of HCl could be achieved only if the total chloride (gas plus aerosol phase) in the system were sufficiently depleted relative to the total sodium. This in turn would imply a lifetime of HCl that was shorter than the lifetime of the chloride-depleted aerosols, which seems possible due to the speed of loss of HCl to the ocean surface and the relatively long lifetime of the submicron aerosols that are most depleted. Aside from these changes in predicted pH and NH_4^+ in the coarse mode, model results were insensitive to minor total chloride depletion. Overall, however, these hypotheses cannot be confirmed since HCl was not measured on the *Discoverer*.

4.1.3. Sensitivity of equilibrium $f(NH_4^+)$. When NH_3 was doubled, an average of 50% of the additional gas was absorbed by the particles (Figure 6). However, this average includes significant additional absorption in the coarse mode in many samples. Considering only the ideal case, where coarse-mode absorption was less, about 30% of the additional gas was absorbed, 20% in the accumulation mode and 10% in the coarse mode.

Equilibrium of the aerosols on the impactor substrates with NH_3 was likely since most particle sampling periods were at least twice as long as the estimated equilibration times (Figure 2). Overall, mean $f(NH_4^+)$ shifted from 0.65 under ambient conditions to 0.45 under sampling conditions (Figure 7), indicating that ~30% of NH_4^+ may have been volatilized during the sampling process. Other model runs indicated that pure $NH_4HSO_4(s)$ solution exhibited negligible volatilization of NH_4^+ when subjected to drying, whereas $NaCl(s)$–$NH_4HSO_4(s)$ solution exhibited ~40% volatilization. Thus the extent of predicted volatilization was heavily dependent upon the assumed degree of internal mixture of the ammonium sulfates with the sea salts in the accumulation mode, and 30% should be considered an upper limit to the possible volatilization.

4.2. Aerosol Equilibration With HNO_3

In all samples, equilibrium NO_3^- was distributed proportionally to sea salt (Figure 8). The common underprediction of NO_3^- in the smallest particles and the consistent overprediction of NO_3^- in the largest particles, combined with the long expected equilibration times of large particles (Figure 2), suggest that the smaller particles were in equilibrium with HNO_3 whereas the largest particles were not.

4.2.1. Accumulation-mode NO_3^-. The aerosols in the accumulation mode had negligible demand for HNO_3 relative to the less acidic sea salts in the coarse mode. However, a significant fraction of NO_3^- was observed in the second size bin in eight samples (samples 27, 30, 33–37, and 45), and was also often measured in the third size bin. Underprediction of accumulation-mode NO_3^- in those samples was caused in part by low HNO_3 predicted at equilibrium due to the absorption of most initial gas by the coarse-mode particles. When the equilibrium of the aerosols in only the three smallest size bins with initial HNO_3 was calculated (in order to prevent absorption by the largest particles), significant NO_3^- was predicted in the third size bin in most samples but still not in the second size bin.

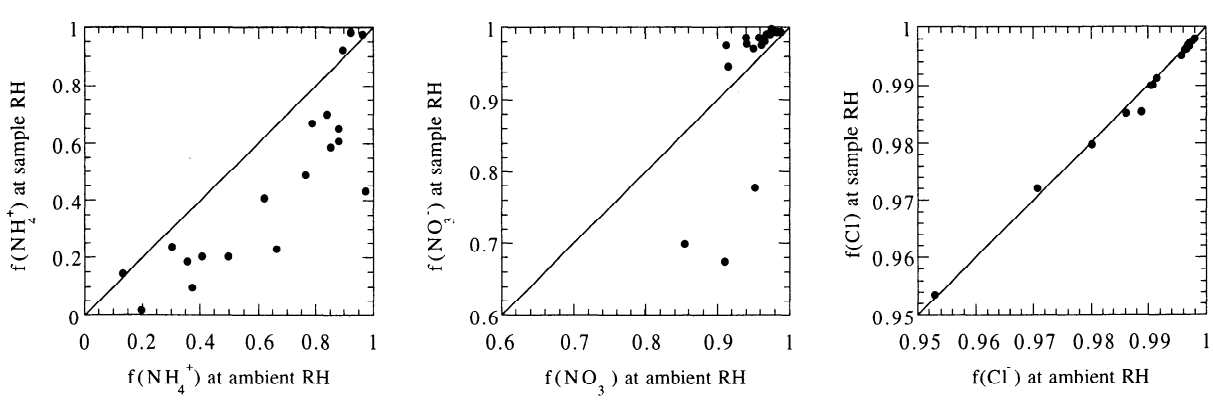

Figure 7. Calculated particulate fraction of ammonium, nitrate, and chloride at sample versus ambient relative humidity. Note varying axis scales.

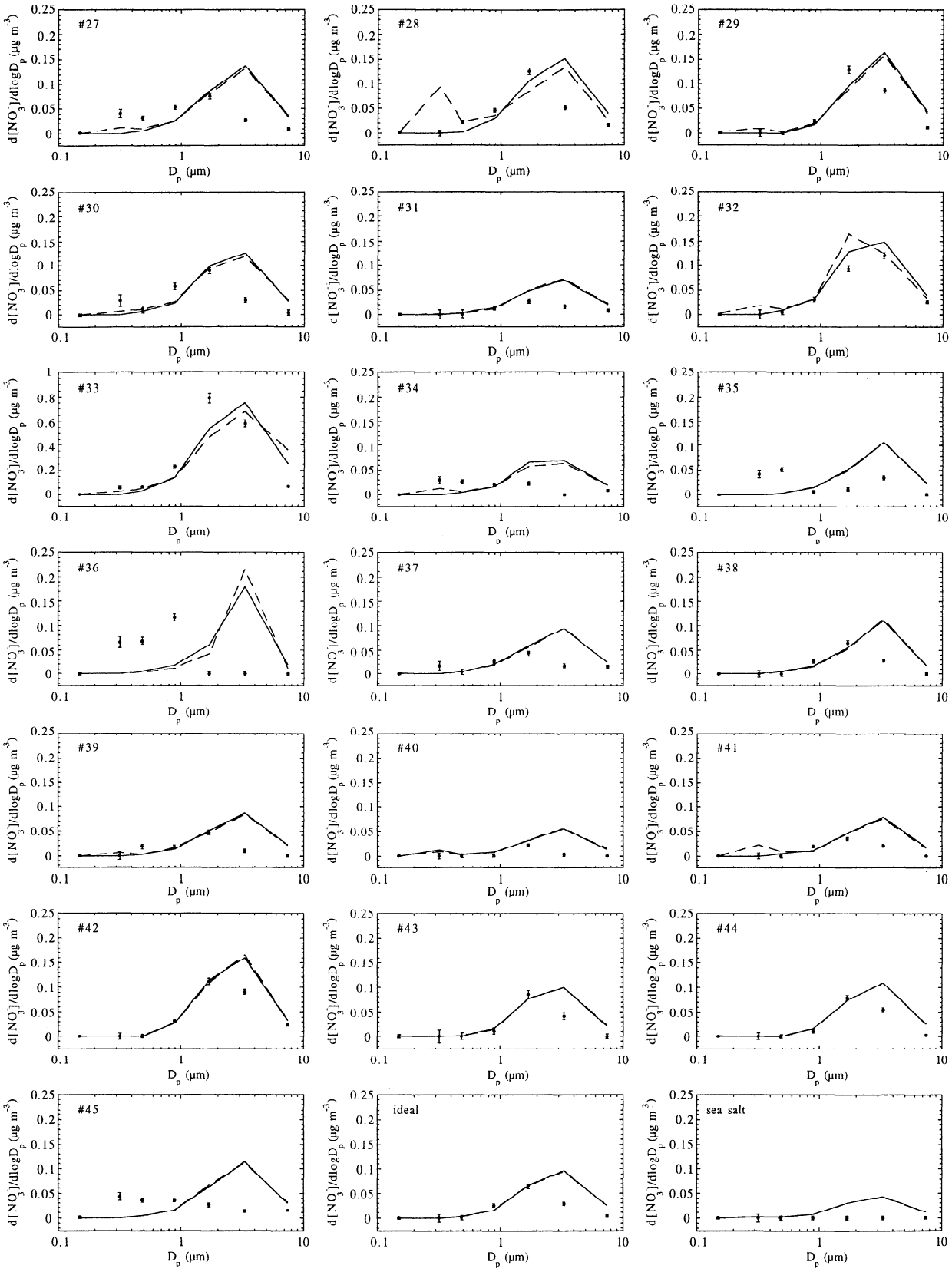

Figure 8. Observed NO_3^- (circles with uncertainty bars) and calculated NO_3^- for charge-imbalanced data (dashed lines) and charge-balanced data (solid lines). Note unique *x* axis scale for sample 33.

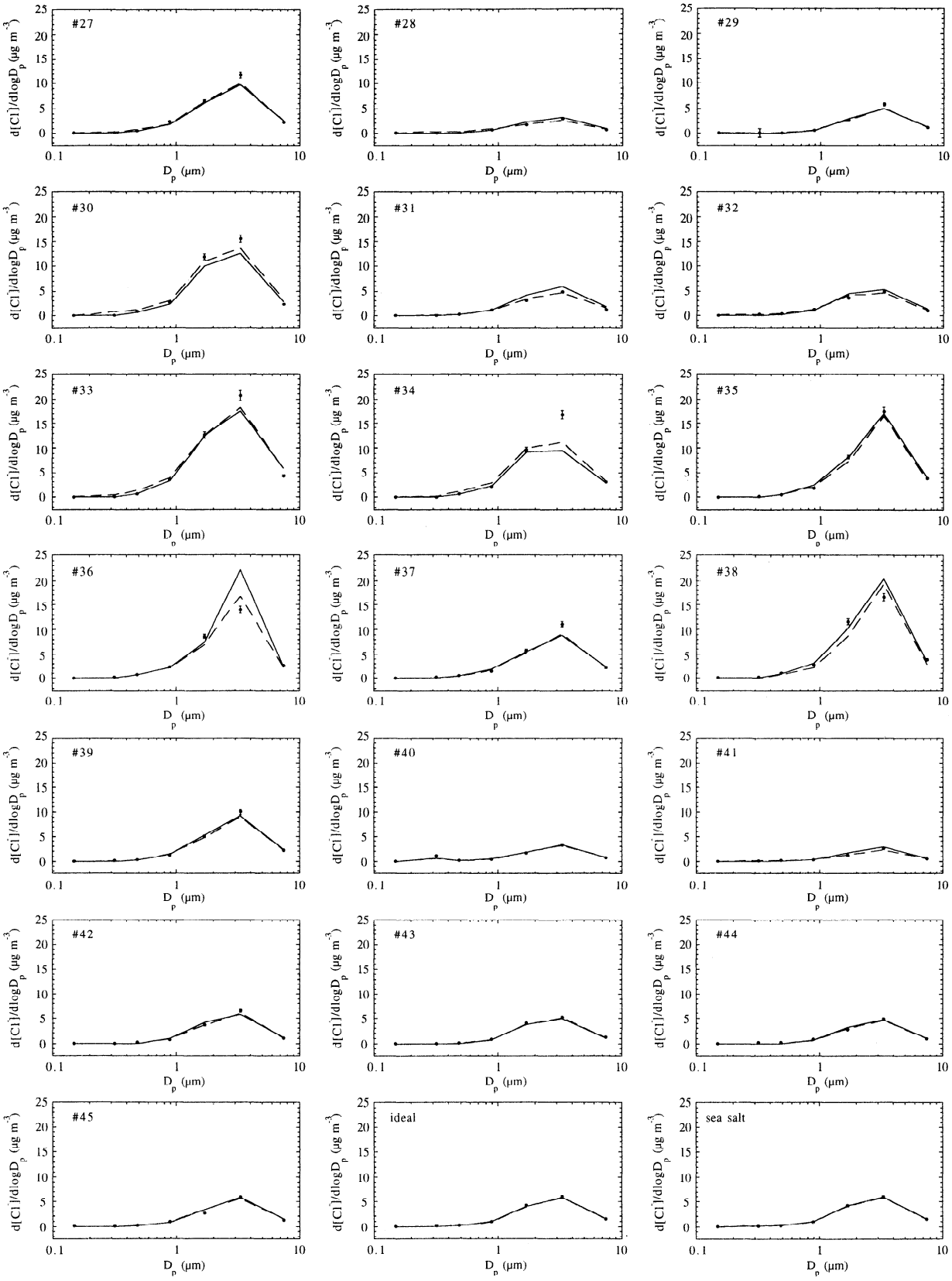

Figure 9. Comparison of observed Cl^- (circles with uncertainty bars) with calculated Cl^- for charge-imbalanced data (dashed lines) and charge-balanced data (solid lines).

Fresh sea spray may have accounted for NO_3^- observed in the second size bin. When $CH_3SO_3^-$ and non-sea-salt SO_4^{2-} were further removed from the three smallest size bins, leaving only nitrate-enriched sea spray, predicted NO_3^- exceeded observations in all three size bins. Thus sufficient sea salt and HNO_3 was present to account for all observed NO_3^- if some degree of external mixture (fresh sea spray) were considered in the accumulation mode. Furthermore, accumulation-mode NO_3^- was highly correlated with sea spray production: seven of the nine samples with peak Cl^- exceeding 10 μg m^{-3} (indicative of recent sea spray production) also exhibited NO_3^- in the second size bin, accounting for all except one such sample.

It is also possible that dust surfaces accounted for the observed NO_3^- in the second size bin, but this seems less likely. Total marine NO_3^- has been previously correlated with continental influence [e.g., *Prospero and Savoie*, 1989]. Of the four samples considered continentally influenced (samples 32–34 and 36), three did exhibit NO_3^- in the second size bin, but this did not account for the remaining majority of such cases. While the charge-balancing process removed the influence of dissolved crustal species, NO_3^- was also underpredicted in the charge-imbalanced case (Figure 8). A mass closure study also indicated that insoluble dust was not a significant component of aerosol mass [*Quinn and Coffman*, 1998].

4.2.2. Coarse-mode NO_3^-. The largest coarse-mode particles did not appear to be at equilibrium with HNO_3. In the two largest size bins, equilibrium NO_3^- always exceeded measured NO_3^-. Furthermore, the discrepancy between the observed and calculated size distributions of NO_3^- was independent of the assumed initial concentration of HNO_3: the equilibrium distribution was always shifted to the larger particles relative to the observed distribution. Observations made under more polluted conditions have indicated that larger sea-salt particles may be subsaturated with HNO_3 relative to micron-sized particles [e.g., *Keene and Savoie*, 1998], and such behavior has also been observed in coastal regions [e.g., *Pakkanen*, 1996]. It has been proposed that this could be due to kinetic transport limitations to equilibrium (e.g., Figure 2) or reaction rate limitations related to the formation and displacement of HCl, but it has not yet been satisfactorily explained [e.g., *Keene et al.*, 1998; *ten Brink*, 1998].

4.2.3. Sensitivity of equilibrium $f(NO_3^-)$. Regardless of initial HNO_3, the sea-salt particles were capable of absorbing almost all available gas (Figure 6), consistent with the results of other modeling studies [e.g., *Keene et al.*, 1998]. When HNO_3 was doubled, an average of 97% of the additional gas was absorbed by the particles. Additionally, equilibrium NO_3^- was always distributed proportionally to sea salt, regardless of the assumed initial concentration of HNO_3.

In most samples the sampling process slightly increased equilibrium $f(NO_3^-)$ due to the decreased pH of the more concentrated aerosol solution remaining after predicted solid formation (Figure 7). No solids contained nitrate, leaving all nitrate in the remaining solution. In three samples (samples 28, 40, and 41), however, the predicted formation of $CaSO_4$–$2H_2O$(s) at the sampling relative humidity in the intermediate size bins decreased the water content sufficiently to significantly lower dissolved NO_3^-. Because of the small number of samples where nitrate partitioning was significantly changed, we conclude that the partitioning of nitrate was generally unchanged by the sampling process.

4.3. Aerosol Equilibration With HCl

The equilibrium size distributions of Cl^- (with estimated HCl) were almost always within the experimental uncertainty of the measurements (Figure 9). Overall, the size distribution of Cl^- was determined primarily by the size distribution of sea-salt cations, which had the greatest demand for the chloride in the system. Sea-salt Cl^- was also displaced as HCl by non-sea-salt sulfate.

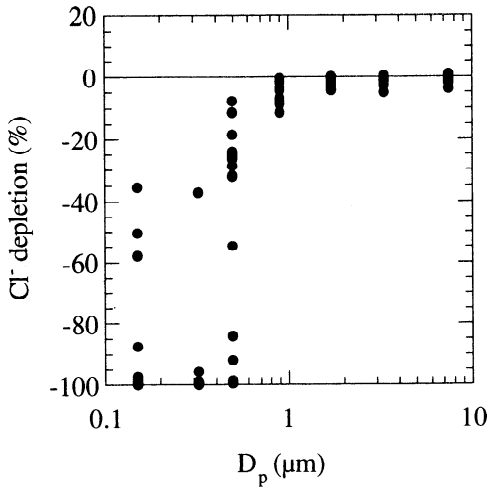

Figure 10. Calculated chloride depletion of charge-balanced samples as a function of aerosol size.

4.3.1. Displacement of Cl^-. Non-sea-salt sulfates were concentrated relative to sea salt in the smallest size bins, resulting in increasing Cl^- depletion with decreasing size (Figure 10). This process depleted a large fraction of the Cl^- present in the smallest size bins (35–100%), but only a small fraction of the total chloride present in the system (0.9–8.5%). The depletion of sea-salt Cl^- from the ideal sample was 3% of the total, consistent with total losses of 0–3% observed in the ACE 1 region [*Ayers et al.*, 1999]. However, the predicted depletion was dependent upon estimated initial HCl and the effect of the charge-balancing procedure on total Cl^-, as well as the assumed degree of internal mixture in the accumulation mode. Uncertainties in these factors precluded quantifying total loss from each sample.

Nonetheless, the pattern of loss from the smallest four size bins was dependent only upon the fact that enrichment by secondary acids was most significant in those size bins. Thus results suggest that most loss would occur even if the largest size bins were not in equilibrium with the ambient gases. The equilibration times in Figure 2 suggest that equilibrium with HCl could have been obtained 2–10 times more quickly than with HNO_3, but the times may still be long for the largest particles. Overall, experimental uncertainty in Cl^- made it impossible to estimate whether individual size bins had obtained equilibrium with HCl, in contrast to the case of nitrate.

4.3.2. Sensitivity of equilibrium $f(Cl^-)$. When HCl was doubled, an average of less than 5% of the additional HCl was taken up by the particles (Figure 6). However, the fact that experimental uncertainty in Cl^- measurements (up to ±25% of 1.5–10.9 μg m^{-3}) may have exceeded any estimate of the gas phase reservoir (100–300 ppt, or 0.15–0.46 μg m^{-3}) made it difficult to draw firm conclusions regarding actual sensitivity to gas concentrations.

Similar to $f(NO_3^-)$, $f(Cl^-)$ was generally unchanged upon aerosol dehydration, an average of less than 1% lower than under ambient conditions (Figure 7). Unlike NO_3^-, however, most Cl^- was predicted in solid forms at the dry sampling relative humidity.

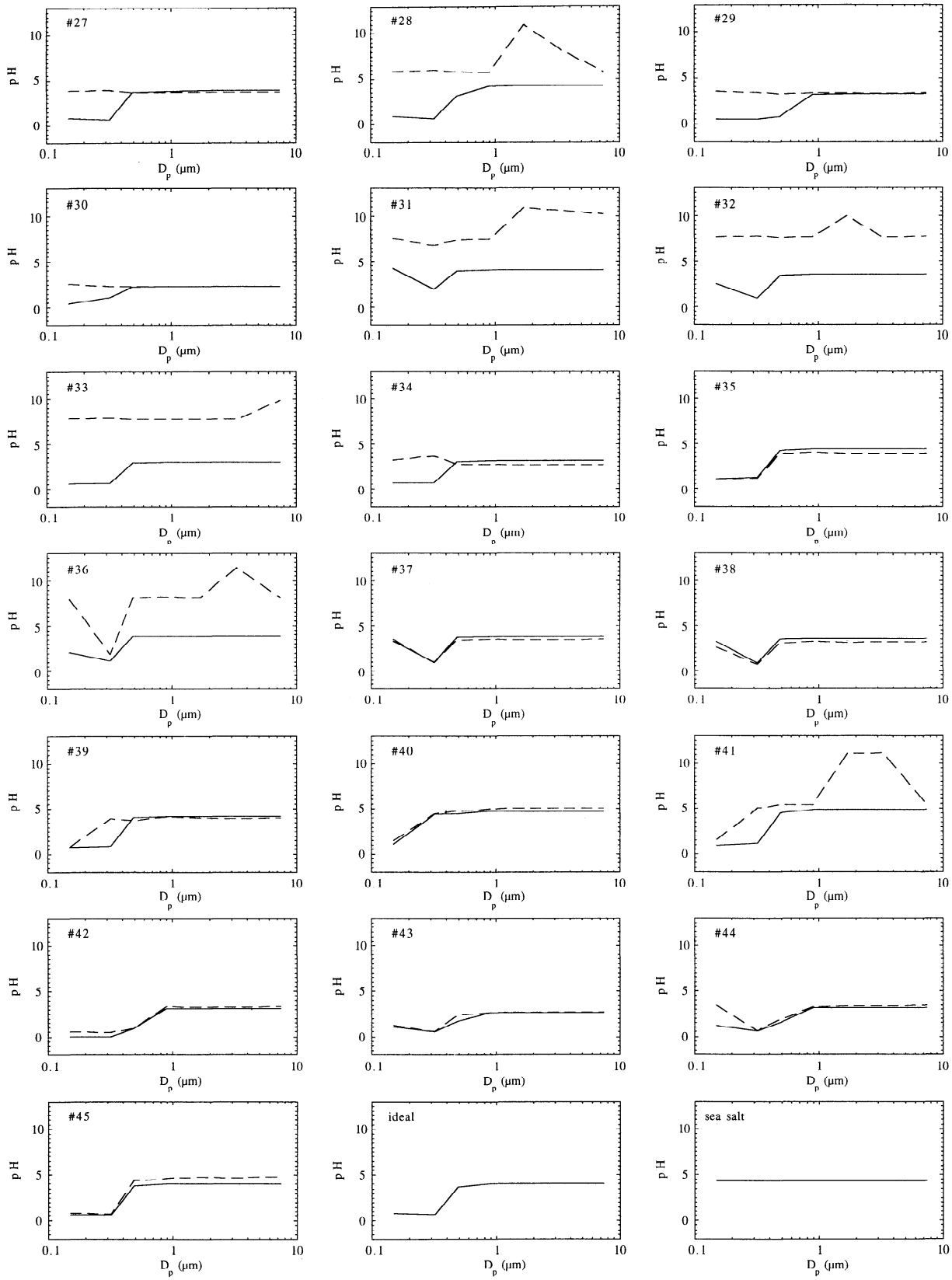

Figure 11. Calculated pH for charge-imbalanced data (dashed lines) and charge-balanced data (solid lines).

4.4. Aerosol pH

In the charge-balanced case, similar pH profiles were predicted in all samples (Figure 11). The larger size bins generally exhibited uniform pH values of 2–5, whereas the first and second size bins generally exhibited lower pH values of 0–2.

4.4.1. Submicron versus supermicron pH. The modeled pH in the submicron size bins was primarily a function of the relative acidity of those size bins (Figure 12). By contrast, the modeled pH of the supermicron size bins was primarily a function of relative humidity (Figure 13). The strong correlation between relative humidity and coarse-mode pH indicates that relative humid-

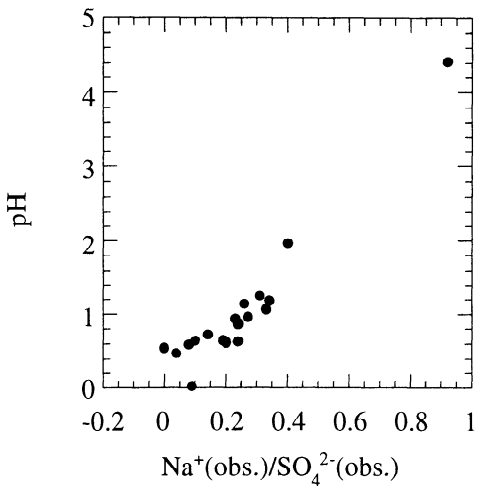

Figure 12. Calculated pH in the 0.32-μm size bin as a function of the ratio of observed Na^+ to SO_4^{2-} in that size bin on a mass basis.

ity controlled the influence of HCl on the modeled sea-salt pH more than either enrichment by secondary acids or the ambient concentration of HCl in the range predicted. The importance of HCl to the pH of sea-salt particles has been noted by previous authors [*Keene and Savoie*, 1998, 1999], as has the importance of relative humidity and liquid water content [*Winkler*, 1986; *Zhu et al.*, 1992].

Whereas the pH of the acidic accumulation-mode particles was a weak increasing function of relative humidity, the pH of the coarse-mode particles was a strong decreasing function of relative humidity. Other runs with prototypical aerosol solutions at typical ACE 1 aerosol and gas concentrations indicated that the pH of NH_4HSO_4(s) solutions increased with increasing relative humidity, regardless of whether the gas-aerosol partitioning of NH_3 was considered. However, the predicted pH of NaCl(s) and NaCl(s)–NH_4HSO_4(s) solutions increased with increasing relative humidity when the gas-aerosol partitioning of HCl was neglected, but decreased with increasing relative humidity when the gas-aerosol partitioning of HCl was considered. Using a model that included HCl partitioning, *Chameides and Stelson* [1992] also predicted decreasing pH of bulk marine aerosols with increasing relative humidity.

4.4.2. Impact of each gas on pH. Overall, modeled equilibrium pH was determined by the composition of the aerosol in each size bin, as well as the interaction with ambient gases. The role of these two influences in the ideal and sea-salt samples was separated by calculating the pH resulting from independent equilibrium with each gas (Figure 14).

When the ideal sample was equilibrated with NH_3 alone, the most acidic size bins were slightly neutralized as initial NH_3 was increased. When equilibrated with HNO_3 alone, the nitric acid was distributed more uniformly relative to sea salt (see Figures 8 and 9), lowering pH in the larger size bins. When equilibrated with HCl alone, the pH of the smallest two size bins remained low, while all of the larger size bins reached a uniform pH that was determined by the interaction with relative humidity and ambient HCl. The small aerosols emitted HCl, raising pH, whereas the larger aerosols absorbed HCl, lowering pH.

Because of the additional importance of relative humidity to sea-salt pH, the equilibrium of HCl with the sea-salt sample was also calculated as a function of relative humidity (Figure 15). The pH was a strong function of relative humidity throughout the range of HCl, but was more weakly dependent upon HCl above approximately 50 ppt. Since most measurements indicate that typical marine HCl levels exceed 50 ppt (see references in section 2.2), these results suggest that relative humidity may be the most important determinant of equilibrium sea-salt pH.

Comparing the equilibrium pH values in Figure 11 with those in Figures 14 and 15 gives insight into the potential pH of non-equilibrium marine particle populations. Freshly emitted sea-salt particles are likely to begin with a pH of 7-9. Interaction with HCl at a given relative humidity may then lower pH to as little as 2, depending upon relative humidity and ambient HCl. Micron-sized sea-salt particles probably reach equilibrium pH, while the largest particles may or may not attain this pH in their lifetimes. Only significant SO_4^{2-} would lower pH further to 0–2, which may occur only for submicron particles.

4.4.3. Comparison with other estimates of pH. In the accumulation mode the pH predicted in this work was generally 0–2, within the range of -1 to 3 that has been previously estimated or observed in clean marine environments (Table 1). In the coarse mode the equilibrium pH predicted here was 2–5, overlapping the range of 3–10 that has been observed or estimated in clean marine environments.

The existing ranges of estimated pH are heavily dependent upon the models that have been applied. In particular, the model treatment and predicted concentration of HCl was found to be critical to the coarse-mode pH estimated here. Of the four models that have been applied to estimate coarse marine aerosol pH in clean environments, *Katoshevski et al.* [1999] did not consider HCl dynamics, obtaining pH values of 6–10, similar to the pH predicted here in fresh sea spray or at very low HCl (Figure 15). The remaining three models did consider the partitioning of HCl, but also predicted higher pH values, consistent with those estimated here at lower HCl concentrations. *Chameides and Stelson* [1992] predicted pH values >8, but did not report HCl; *Erickson et al.* [1999] predicted pH values of 5–8 and <50 ppt HCl; and *Vogt et al.* [1996] predicted pH values of 5–6 and 0–20 ppt HCl at 76% relative humidity. In summary, the equilibrium coarse-mode pH values predicted in this work appear to be consistent with other estimates when the role of HCl is considered.

5. Conclusions

The gas-aerosol partitioning of ammonium, nitrate, and chloride during the ACE 1 experiment was analyzed by comparing

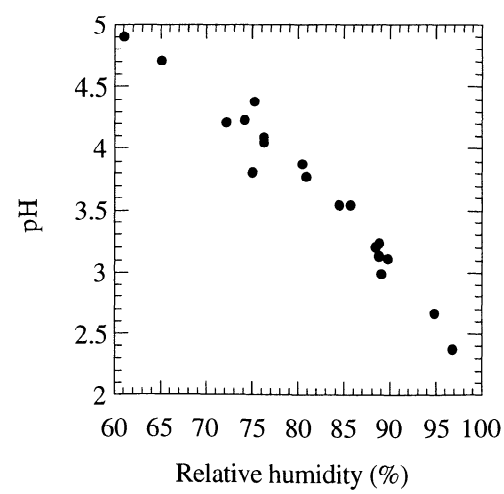

Figure 13. Calculated pH in the 3.4-μm size bin as a function of ambient relative humidity.

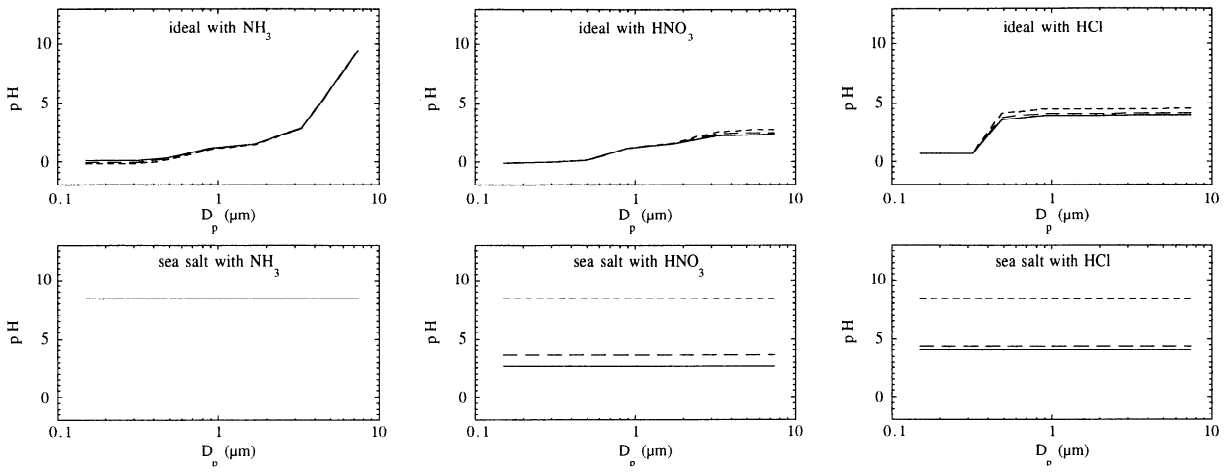

Figure 14. Calculated pH of ideal and pure sea-salt samples in equilibrium independently with NH_3, HNO_3, and HCl at initial gas concentrations of zero (dotted lines), the observed or estimated values (dashed lines), and double the observed or estimated values (solid lines).

equilibrium model results with measurements. The above analysis supports the following general conclusions:

1. All aerosols appeared likely to be in equilibrium with NH_3 based on comparison of observations with predictions and analysis of gas-aerosol equilibration times. Particles were sensitive to increased NH_3, absorbing at least 20% of additional gas when initial NH_3 was doubled. Model results indicated that up to 30% of NH_4^+ present under ambient conditions may have been volatilized during the sampling process.

2. Submicron and micron-sized aerosols were likely in equilibrium with HNO_3, but the largest particles appeared to be undersaturated. Particles were sensitive to increased HNO_3 and were capable of absorbing essentially all additional gas when initial HNO_3 was doubled.

3. Smaller particles appeared likely to be in equilibrium with HCl, whereas larger particles may or may not have been, based upon calculated gas-aerosol equilibration times. Emission of HCl due to displacement by secondary acids was probably nearly complete (close to equilibrium) since secondary acids were concentrated in the smallest particles and the smallest particles were likely to achieve equilibrium quickly.

4. The estimated equilibrium pH of the accumulation-mode aerosols was 0–2, whereas the estimated equilibrium pH of the coarse-mode aerosols was 2–5. The pH of sea spray may have varied in the range of 7–9 for fresh particles down to 2 for aged particles at high relative humidity and high HCl. Under ACE 1 conditions the modeled equilibrium pH of the accumulation-mode particles was primarily a function of the amount of sulfates present relative to sea salt. By contrast, the modeled equilibrium pH of the coarse-mode particles was primarily a function of HCl concentration and relative humidity.

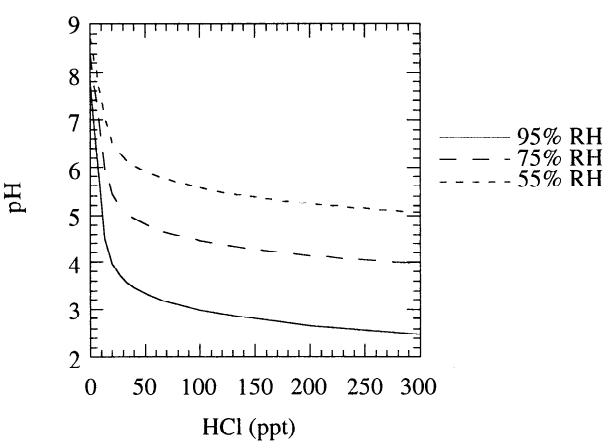

Figure 15. Calculated pH of the sea-salt sample as a function of initial HCl and relative humidity.

While it was possible to draw conclusions from the available data based on the results of sensitivity tests, the model remained unconstrained by the observations in several important ways. With respect to accumulation-mode pH and NH_3 equilibrium, the model was sensitive to assumptions regarding aerosol mixing state. Hygroscopicity data gathered on the *Discoverer* at 0.165 μm indicated that an external mixture was often present at that diameter, but no data were gathered at larger sizes [*Berg et al.*, 1998]. Additional data on aerosol mixing state up to at least 1 μm in diameter would have provided an important model constraint. With respect to coarse-mode pH and HNO_3 and HCl equilibrium, data for both gas species would clearly have provided important constraints. Constraining chlorine is complicated by the fact that coarse-mode aerosol pH may be quite sensitive to HCl, but the total chlorine in the system is dominated by Cl^-, which probably cannot be measured more precisely without sacrificing time and size resolution of the aerosol measurements.

Acknowledgments. This material is based upon work supported under a National Science Foundation Graduate Fellowship, National Science Foundation agreements ATM-9504481 and ATM-9614118, and National Aeronautics and Space Administration agreement NIP-0000-0003. We are grateful to the following researchers for providing ACE 1 data: Patricia Quinn (particle ionic mass and NH_3 data), Timothy Bates and James Johnson (meteorological and radon data), and Richard Feely (CO_2 data).

References

Abbatt, J. P. D., and G. C. G. Waschewsky, Heterogeneous interactions of HOBr, HNO_3, and NO_2 with deliquescent NaCl aerosols at room temperature, *J. Phys. Chem. A, 102*, 3719–3725, 1998.

Allen, A. G., A. L. Dick, and B. M. Davison, Sources of atmospheric methanesulphonate, non-sea-salt sulphate, nitrate, and related species over the temperate South Pacific, *Atmos. Environ.*, *31*, 191–205, 1997.

Ayers, G. P., R. W. Gillett, J. M. Cainey, and A. L. Dick, Chloride and bromide loss from sea-salt particles in Southern Ocean air, *J. Atmos. Chem.*, *33*, 299–319, 1999.

Barger, W. R., and W. D. Garrett, Surface active organic material in the marine atmosphere, *J. Geophys. Res.*, *75*, 4561–4566, 1970.

Bates, T. S., B. J. Huebert, J. L. Gras, F. B. Griffiths, and P. A. Durkee, International Global Atmospheric Chemistry (IGAC) Project's First Aerosol Characterization Experiment (ACE 1): Overview, *J. Geophys. Res.*, *103*, 16,297–16,318, 1998a.

Bates, T. S., V. N. Kapustin, P. K. Quinn, D. S. Covert, D. J. Coffman, C. Mari, P. A. Durkee, W. J. DeBruyn, and E. S. Saltzman, Processes controlling the distribution of aerosol particles in the lower marine boundary layer during the First Aerosol Characterization Experiment (ACE 1), *J. Geophys. Res.*, *103*, 16,369–16,383, 1998b.

Berg, O. H., E. Swietlicki, and R. Krejci, Hygroscopic growth of aerosol particles in the marine boundary layer over the Pacific and Southern Oceans during the First Aerosol Characterization Experiment (ACE 1), *J. Geophys. Res.*, *103*, 16,535–16,545, 1998.

Chameides, W. L., and A. W. Stelson, Aqueous-phase chemical processes in deliquescent sea-salt aerosols: A mechanism that couples the atmospheric cycles of S and sea salt, *J. Geophys. Res.*, *97*, 20,565–20,580, 1992.

Clegg, N. A., and R. Toumi, Sensitivity of sulphur dioxide oxidation in sea salt to nitric acid and ammonia gas phase concentrations, *J. Geophys. Res.*, *102*, 23,241–23,249, 1997.

Clegg, S. L., and P. Brimblecombe, The solubility of methanesulphonic acid and its implications for atmospheric chemistry, *Environ. Technol. Lett.*, *6*, 269–278, 1985.

Clegg, S. L., P. B. Brimblecombe, and A. S. Wexler, Thermodynamic model of the system H^+–NH_4^+–Na^+–SO_4^{2-}–NO_3^-–Cl^-–H_2O at 298.15 K, *J. Phys. Chem.*, *102*, 2155–2171, 1998.

Covington, A. K., R. A. Robinson, and R. Thompson, Osmotic and activity coefficients for aqueous methane sulfonic acid solutions at 25°C, *J. Chem. Eng. Data*, *18*, 422-423, 1973.

Erickson, D. J., III, C. Seuzaret, W. C. Keene, and S. L. Gong, A general circulation model based calculation of HCl and $ClNO_2$ production from sea-salt dechlorination: Reactive Chlorine Emissions Inventory, *J. Geophys. Res.*, *104*, 8347–8372, 1999.

Fitzgerald, J. W., Marine aerosols: A review, *Atmos. Environ., Part A*, *25*, 533–545, 1991.

Graedel, T. E., and W. C. Keene, Tropospheric budget of reactive chlorine, *Global Biogeochem. Cycles*, *9*, 47–77, 1995.

Gras, J. L., and G. P. Ayers, Marine aerosol at midlatitudes, *J. Geophys. Res.*, *88*, 10,661–10,666, 1983.

Horvath, H., Atmospheric light absorption—A review, *Atmos. Environ., Part A*, *27*, 293–317, 1993.

Jacob, D., Comment on "The photochemistry of a remote stratiform cloud" by William Chameides, *J. Geophys. Res.*, *90*, 5864, 1985.

Jacobson, M. Z., *Fundamentals of Atmospheric Modeling*, 656 pp., Cambridge University Press, New York, 1999a.

Jacobson, M. Z., Studying the effects of calcium and magnesium on size-distributed nitrate and ammonium with EQUISOLV II, *Atmos. Environ.*, *33*, 3635–3649, 1999b.

Jones, A., and A. Slingo, Climate model studies of sulfate aerosols and clouds, *Philos. Trans. R. Soc. London, Ser. B*, *352*, 221–228, 1997.

Kajii, Y., H. Akimoto, Y. Komazaki, S. Tanaka, H. Mukai, K. Murano, and J. T. Merrill, Long-range transport of ozone, carbon monoxide, and acidic trace gases at Oki Island, Japan, during PEM-West B/PEACAMPOT B campaign, *J. Geophys. Res.*, *102*, 28,637–28,649, 1997.

Katoshevski, D., A. Nenes, and J. H. Seinfeld, A study of processes that govern the maintenance of aerosols in the marine boundary layer, *J. Aerosol Sci.*, *30*, 503–532, 1999.

Keene, W. C., and D. L. Savoie, The pH of deliquesced sea-salt aerosol in polluted marine air, *Geophys. Res. Lett.*, *25*, 2181–2184, 1998.

Keene, W. C., and D. L. Savoie, Correction to "The pH of deliquesced sea-salt aerosol in polluted marine air," *Geophys. Res. Lett.*, *26*, 1315–1316, 1999.

Keene, W. C., J. R. Maben, A. A. P. Pszenny, and J. N. Galloway, Measurement technique for inorganic chlorine gases in the marine boundary layer, *Environ. Sci. Technol.*, *27*, 866–874, 1993.

Keene, W. C., R. Sander, A. A. P. Pszenny, R. Vogt, P. J. Crutzen, and J. N. Galloway, Aerosol pH in the marine boundary layer: A review and model evaluation, *J. Aerosol Sci.*, *29*, 339–356, 1998.

Kreidenweis, S. M., L. M. McInnes, and F. J. Brechtel, Observations of aerosol volatility and elemental composition at Macquarie Island during the First Aerosol Characterization Experiment (ACE 1), *J. Geophys. Res.*, *103*, 16,511–16,524, 1998.

Matsumoto, K., I. Nagao, H. Tanaka, H. Miyaji, T. Iida, and Y. Ikebe, Seasonal characteristics of organic and inorganic species and their size distributions in atmospheric aerosols over the northwest Pacific Ocean, *Atmos. Environ.*, *32*, 1931–1946, 1998.

McInnes, L. M., D. S. Covert, P. K. Quinn, and M. S. Germani, Measurements of chloride depletion and sulfur enrichment in individual sea-salt particles collected from the remote marine boundary layer, *J. Geophys. Res.*, *99*, 8257–8268, 1994.

Meng, Z., and J. H. Seinfeld, Time scales to achieve atmospheric gas-aerosol equilibrium for volatile species, *Atmos. Environ.*, *30*, 2889–2900, 1996.

Middlebrook, A. M., D. M. Murphy, and D. S. Thomson, Observations of organic material in individual marine particles at Cape Grim during the First Aerosol Characterization Experiment (ACE 1), *J. Geophys. Res.*, *103*, 16,475–16,483, 1998.

Murphy, D. M., J. R. Anderson, P. K. Quinn, L. M. McInnes, F. J. Brechtel, S. M. Kreidenweis, A. M. Middlebrook, M. Pósfai, D. S. Thomson, and P. R. Buseck, Influence of sea-salt on aerosol radiative properties in the Southern Ocean marine boundary layer, *Nature*, *392*, 62–65, 1998.

O'Dowd, C. D., M. H. Smith, I. E. Consterdine, and J. A. Lowe, Marine aerosol, sea-salt, and the marine sulphur cycle: A short review, *Atmos. Environ.*, *31*, 73–80, 1997.

Pakkanen, T. A., Study of formation of coarse particle nitrate aerosol, *Atmos. Environ.*, *30*, 2475–2482, 1996.

Papenbrock, T., F. Stuhl, K. P. Müller, and J. Rudolph, Measurement of gaseous HNO_3 over the Atlantic Ocean, *J. Atmos. Chem.*, *15*, 369–379, 1992.

Parungo, F. P., C. T. Nagamoto, J. Rosinski, and P. L. Haagenson, A study of marine aerosols over the Pacific Ocean, *J. Atmos. Chem.*, *4*, 199–226, 1986.

Pósfai, M., J. R. Anderson, and P. R. Buseck, Compositional variations of sea-salt-mode aerosol particles from the North Atlantic, *J. Geophys. Res.*, *100*, 23,063–23,074, 1995.

Prospero, J. M., and D. L. Savoie, Effect of continental sources on nitrate concentrations over the Pacific Ocean, *Nature*, *339*, 687–689, 1989.

Pszenny, A. A. P., W. C. Keene, D. J. Jacob, S. Fan, J. R. Maben, M. P. Zetwo, M. Springer-Young, and J. N. Galloway, Evidence of inorganic chlorine gases other than hydrogen chloride in marine surface air, *Geophys. Res. Lett.*, *20*, 699–702, 1993.

Quinn, P. K., and D. J. Coffman, Local closure during the First Aerosol Characterization Experiment (ACE 1): Aerosol mass concentration and scattering and backscattering coefficients, *J. Geophys. Res.*, *103*, 16,575–16,596, 1998.

Quinn, P. K., and D. J. Coffman, Comment on "Contribution of different aerosol species to the global aerosol extinction optical thickness: Estimates from model results" by I. Tegen et al., *J. Geophys. Res.*, *104*, 4241–4248, 1999.

Quinn, P. K., W. E. Asher, and R. J. Charlson, Equilibria of the marine multiphase ammonia system, *J. Atmos. Chem.*, *14*, 11–30, 1992.

Quinn, P. K., D. J. Coffman, V. N. Kapustin, T. S. Bates, and D. S. Covert, Aerosol optical properties in the marine boundary layer during the First Aerosol Characterization Experiment (ACE 1) and the underlying chemical and physical aerosol properties, *J. Geophys. Res.*, *103*, 16,547–16,563, 1998.

Sander, R., and P. J. Crutzen, Model study indicating halogen activation and ozone destruction in polluted marine air masses transported to the sea, *J. Geophys. Res.*, *101*, 9121–9138, 1996.

Seinfeld, J. H., and S. N. Pandis, *Atmospheric Chemistry and Physics*, 1326 pp., John Wiley, New York, 1998.

Sievering, H., J. Boatman, E. Gorman, Y. Kim, L. Anderson, G. Ennis, M. Luria, and S. Pandis, Removal of sulphur from the marine boundary layer by ozone oxidation in sea-salt aerosols, *Nature*, *360*, 571–573, 1992.

Singh, H. B., Halogens in the atmospheric environment, in *Composition, Chemistry, and Climate of the Atmosphere*, edited by H. B. Singh, pp. 216–250, Van Nostrand Reinhold, New York, 1995.

Slinn, S. A., and W. G. N. Slinn, Predictions for particle deposition on natural waters, *Atmos. Environ.*, *14*, 1013-1016, 1980.

Stumm, W., and J. J. Morgan, *Aquatic Chemistry*, 1022 pp., John Wiley, New York, 1996.

Swartz, E., Q. Shi, P. Davidovits, J. T. Jayne, D. R. Worsnop, and C. E. Kolb, Uptake of gas-phase ammonia. 2. Uptake by sulfuric acid surfaces, *J. Phys. Chem. A*, *103*, 8824–8833, 1999.

ten Brink, H. M., Reactive uptake of HNO_3 and H_2SO_4 in sea-salt (NaCl) particles, *J. Aerosol Sci.*, *29*, 57-64, 1998.

Vogt, R., P. J. Crutzen, and R. Sander, A mechanism for halogen release from sea-salt aerosol in the remote marine boundary layer, *Nature*, *383*, 327–329, 1996.

Whittlestone, S., J. L. Gras, and S. T. Siems, Surface air mass origins during the First Aerosol Characterizations Experiment (ACE 1), *J. Geophys. Res.*, *103*, 16,341–16,350, 1998.

Winkler, P., Relations between aerosol acidity and ion balance, in *Chemistry of Multiphase Atmospheric Systems*, edited by W. Jaeschke, pp. 269–298, Springer-Verlag, New York, 1986.

Zhang, Y., C. Seigneur, J. H. Seinfeld, M. Z. Jacobson, S. L. Clegg, and F. S. Binkowski, A comparative review of inorganic aerosol thermodynamic equilibrium modules: Similarities, differences, and their likely causes, report, Coord. Res. Counc., Inc., Atlanta, Ga., 1998.

Zhu, X., J. M. Prospero, F. J. Millero, D. L. Savoie, and G. W. Brass, The solubility of ferric ion in marine mineral aerosols at ambient relative humidities, *Mar. Chem.*, *38*, 91–107, 1992.

A. M. Fridlind and M. Z. Jacobson, Department of Civil and Environmental Engineering, Stanford University, Stanford, CA 94305-4020. (fridlind@stanford.edu; jacobson@ce.stanford.edu)

(Received November 1, 1999; revised March 24, 2000; accepted March 28, 2000.)